Enabling Reflective & Refractive Depth Representation in Computer-Generated Holography

Aaron Demolder
Hammadi Nait-Charif
Valery Adzhiev
Bournemouth University
Bournemouth, UK

Alfred Newman
Tom Durrant
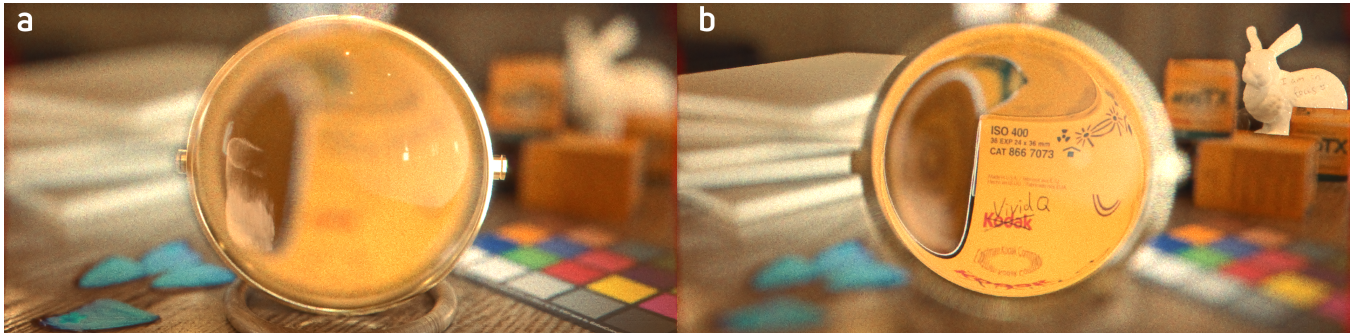Andrzej Kaczorowski
VividQ Ltd
Cambridge, UK

Figure 1: Holographic replays (simulated) of a scene containing a lens of f=180mm, 0.5m from camera. (a) Focus is at 0.46m on the smudge, reflection focus of lights is 0.52m. (b) Focus (1m) now on the text and bunny, the film box is 150mm behind the lens.

1 INTRODUCTION

Computer-Generated Holography (CGH) is a technique for the reconstruction and display of three-dimensional imagery through diffraction and interference of light. Holograms are generated digitally by calculating light propagation, and displayed on devices called Spatial Light Modulators (SLMs). When illuminated by coherent laser light, holograms then replay a full 3D scene. Recently, holography has received significant attention from industrial and academic communities, with neural holography [Peng et al. 2020] [Shi et al. 2021] and numerous other techniques [Sahin et al. 2020]. Applications of holography include Augmented/Virtual Reality [Widjanarko et al. 2020], Head-Up Displays, and larger display devices [An et al. 2020]. In the real world, objects can be viewed in reflections (such as mirrors) and through refractions (such as glass or water); the depth at which these objects focus is defined by the focal power of the material. In computer graphics, realistic

representation of materials is essential to the realism of the image. These effects do not pose an issue for 2D display, as only the pixel intensities are required while focus is pre-determined. By contrast, in image/layer-based holography, z-depth values are used that correspond to the focus distance of objects. While this technique works well for the first object hit by the raytracer, it is unable to accurately encode the depth at which virtual objects appear after reflection or refraction. It is hence necessary for the renderer to pass multiple depth values to the hologram generation engine to ensure realistic representation of reflections and refractions in a realistic 3D display.

2 APPROACH

We propose a method of utilising additional depth information required for reflective and refractive material representations on holographic displays via multiple render passes, and a first-of-its-kind method of multi-pass holographic compositing whereby render passes are combined in the hologram (frequency) domain. The resulting hologram successfully represents the input render, but now with the correct depth information for all render passes supplied. The resulting hologram can consequently be displayed on an SLM and viewed by eye with the correct perceptual cues, resulting in correct focus properties (see Figure 1).

3 IMPLEMENTATION

The 'depth' of a point refers to the distance from which multiple rays from that point appear to diverge. In the case of an object being viewed in the reflection of a flat mirror, the total depth is the length from the object to the mirror and then to the viewer. Figure 2(a) shows the primary ray from viewer to mirror, and a secondary ray [Whitted 1980] from mirror to object. A z-depth pass will provide the length of only the primary ray, so must be added to the length
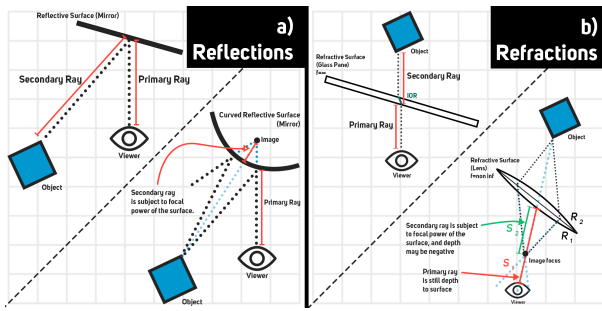
Figure 2: (a) The total depth required for reflections is the summation of primary and secondary rays, following the law of reflection. (b) The focal length is calculated with the Index of Refraction (IOR) given by Snell's Law, and the thickness of the material. A material may exhibit both reflective and refractive properties simultaneously.
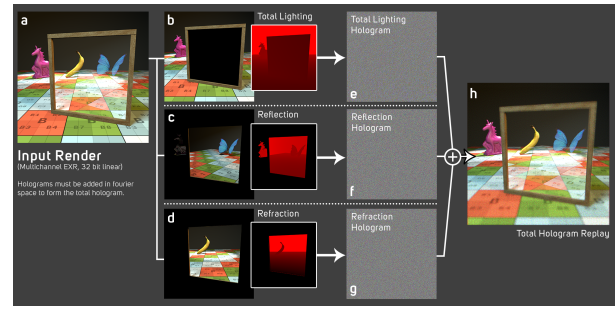

Figure 3: (a) The input multichannel file. (b) Total Lighting render, z-depth. (c) Reflection render, associated depth. (d) Refraction render, associated depth. (e) Hologram of Total Lighting only. (f) Hologram of Reflection only. (g) Hologram of Refraction Only. (h) The total composite hologram replay, via a plus operation of the holograms for each render pass.

of the reflection secondary ray for the correct depth of the object in camera space. A refraction depth pass is performed in a similar fashion, as seen in Figure 2(b). In the case of looking through glass, the primary ray is formed by the depth from viewer to the surface of the glass, but the length of the secondary ray is determined by the shape of the surface as well as the refractive index. The resulting image may be real or virtual, and have magnification. The focal length of the lens is given by the lensmaker's equation:

$$\frac{1}{f} = (n - 1) \left(\frac{1}{R_1} - \frac{1}{R_2} \right) \quad (1)$$

Where f is focal length, n is Index of Refraction (IOR) and R_1, R_2 are the radii of curvature of the surface. The new secondary ray depth of the object image visible through the lens is given by:

$$\frac{1}{S_2} = \frac{1}{f} - \frac{1}{S_1} \quad (2)$$

Where S_1 and S_2 are the depths to the lens and the object respectively. When added, S_1 and S_2 provide the total correct depth value. Most renderers will already store a value for focus depth per pixel per render pass. Each colour pass can still be adjusted as required in compositing software. The resulting passes can then be loaded for hologram generation - here we employ VividQ's Software Development Kit. The resulting outputs are images in Fourier space (where the image is decomposed into its constituent frequencies) for each render pass which can be displayed on a holographic projector. As holograms are additive in the same way light is - each of the holograms can consequently be composited using a familiar multi-pass process. Whilst still in frequency space, each of the holograms are combined, shown in Figure 3. When displayed on an SLM, this will 'replay' the 3D scene to the viewer, with the correct material depth information.

4 CONCLUSIONS

The results shown in both Figure 1 and Figure 4 demonstrate that the methods introduced represent a significant step towards realistic imagery for holographic display, with physically correct reflections and refractions - whilst remaining fully compatible with the current computer graphics pipeline. However, Image-based hologram generation methods result in black artefacts in a scene, as no colour data exists behind each depth layer – this is visible when objects defocus. This could be minimised by including data that
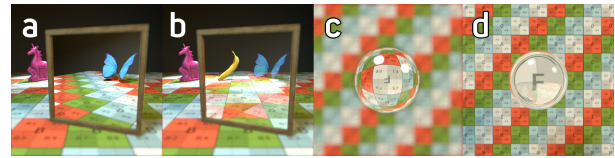

Figure 4: (a) Replay of butterfly reflection and unicorn (both 9m) (b) Changing the mirror to glass reveals a banana (9m). (c) Grid at 1m from camera focused by a lens (f=100mm) placed 850mm from the camera, the grid focuses at 550mm (real). Reflection focus is 950mm. (d) Grid at 1m from camera focused by a lens (f=100mm) placed 950mm from the camera, the grid focuses at 1050mm (virtual). Reflection focus is 1050mm.

allows object-based and render-pass-based overscan for objects that are occluded. For best results this data would be sourced directly from the renderer, but estimates could be made with object based AOVs (such as cryptomatte [Friedman and Jones 2015] or object ID manifests [Hillman 2018]) by generating dilated edges per object.

ACKNOWLEDGMENTS

REFERENCES

Jungkwuen An, Kanghee Won, Young Kim, Jong-Young Hong, Hojung Kim, Yongkyu Kim, Hoon Song, Chilsung Choi, Yunhee Kim, Juwon Seo, Alexander Morozov, Hyunsik Park, Sunghoon Hong, Sungwoo Hwang, Kichul Kim, and Hong-Seok Lee. 2020. Slim-panel holographic video display. *Nature Communications* 11, 1 (2020). https://doi.org/10.1038/s41467-020-19298-4

Jonah Friedman and Andrew C. Jones. 2015. Fully Automatic ID Mattes with Support for Motion Blur and Transparency. In *ACM SIGGRAPH 2015 Posters (SIGGRAPH '15)*. Article 47. https://doi.org/10.1145/2787626.2787629

Peter Hillman. 2018. A Scheme for Storing Object ID Manifests in OpenEXR Images. In *Proceedings of the 8th Annual Digital Production Symposium (DigiPro '18)*. Article 9. https://doi.org/10.1145/3233085.3233086

Yifan Peng, Suyeon Choi, Nitish Padmanaban, and Gordon Wetzstein. 2020. Neural Holography with Camera-in-the-Loop Training. *ACM Trans. Graph.* 39, 6, Article 185 (2020). https://doi.org/10.1145/3414685.3417802

Erdem Sahin, Elena Stoykova, Jani Mäkinen, and Atanas Gotchev. 2020. Computer-Generated Holograms for 3D Imaging: A Survey. *ACM Comput. Surv.* 53, 2, Article 32 (2020). https://doi.org/10.1145/3378444

Liang Shi, Beichen Li, Changil Kim, Petr Kellnhofer, and Wojciech Matusik. 2021. Towards real-time photorealistic 3D holography with deep neural networks. *Nature* 591, 7849 (2021). https://doi.org/10.1038/s41586-020-03152-0

Turner Whitted. 1980. An Improved Illumination Model for Shaded Display. *Commun. ACM* 23, 6 (1980). https://doi.org/10.1145/358876.358882

T. Widjanarko, M. El Guendy, A. O. Spiess, D. M. Sullivan, T. J. Durrant, O. A. Tastemur, A. J. Newman, D. F. Milne, and A. Kaczorowski. 2020. Clearing key barriers to mass adoption of augmented reality with computer-generated holography. In *Optical Architectures for Displays and Sensing in Augmented, Virtual, and Mixed Reality (AR, VR, MR)*, Vol. 11310. SPIE. https://doi.org/10.1117/12.2544979